Investigation of the electron plasma component produced by some types of gas-discharge arc sources

E. V. Shun'ko
University of Pittsburgh, Pittsburgh, Pennsylvania 15260
(Received 31 May 1991; revised manuscript received 16 December 1991)

Parameters of an electron component of plasma produced by two types of the gas-discharge arc sources (V. I. Davidenko *et al.*, Sov. Phys.—Tech. Phys. **28**, 160 (1983) [Zh. Tekh. Fiz. **53**, 258 (1983)]; G. I. Dimov, A. A. Ivanov, and G. V. Roslyakov, Sov. J. Plasma Phys. **8**, 546 (1982) [Fiz. Plazmy **8**, 970 (1982)]) are given. An analysis is made of the hypothesis [E. V. Shun'ko, Phys. Lett. A **147**, 37 (1990)] that under special conditions, related to the configurations of these sources, the isotropic thermal motion of plasma electrons is stratified into separate localized electron currents due to a filamentation, its mechanism being similar to the current instability.

PACS number(s): 52.80.Tn, 52.25.Fi, 52.80.Mg

I. INTRODUCTION

The investigation of some types of gas-discharge arc sources [1,2] enables one to infer that the isotropic thermal motion of electrons in plasma produced by these sources is stratified into the separate localized currents (filaments). One can also infer that the instability resulting in the filamentation is similar in its nature to the current one [3]. This hypothesis is based on the study of I-V characteristics of a cylindrical Langmuir probe in a plasma with electron flow [4], and it is both of theoretical and practical interest since these types of sources are used as the plasma generators for preparing target plasma in experimental thermonuclear installation [5] as well as for obtaining the positive and negative hydrogen ions for different technological applications [6]. Therefore, the basic experimental data and the technique of their processing should be considered in detail.

In the general series of experiments at the plasma source [1] there were used the special thermionically cleaned probes [7]. The traditional measurement procedure was applied here, i.e., a pulsed voltage scanning generator with a double-differentiation current circuit [8] was connected through one of its poles to the probe, and through the other one to a metallic vacuum chamber contacting with the plasma. Such a procedure of measurements turned out to be applicable due to the high stability of plasma parameters of the source in the process of the injection pulse.

We will make the assumption that the probe was likely interacting with the thermal electron flows [4] for which $v_d/\langle v\rangle > 1$ and check this hypothesis later. Here v_d is the averaged over the ensemble drift velocity of the flow motion, and $\langle v\rangle$ is the average thermal electron velocity in the system of the flow motion. But the technique of the reconstruction of the probe-unperturbed plasma parameters by the I-V characteristics of the real probe was in fact formulated only for the case when $v_d/\langle v\rangle \ll 1$ [9]. For extending this technique to the region $v_d/\langle v\rangle > 1$, special investigations were performed which aimed at comparing plasma parameters obtained from two probes of different diameters [9]. Thus, a pair of probes, one of 5-μm and another of 26-μm diameters and each ~ 3 mm long, was inserted into plasma. The probes were mounted on the common console parallel to one another at a distance ~ 1 mm. This made it possible to perform, by the movable probe pair, the simultaneous measurements of the wide range of plasma parameters using their natural variation with the distance from the source. Unless otherwise specified, all the measurements were performed for the probe axes orthogonal to the source axis and with the magnetic field of the source switched off.

II. THEORY OF CYLINDRICAL PROBE IN PLASMA WITH FILAMENTED ELECTRONS

As has been shown, the electron-distribution function is Maxwellian in the system of motion for each of the flows considered and we shall use the expressions derived formerly for this Maxwellian distribution function [4].

As has been found, the current on the probe is a current sum from the electron flows integrated over the whole solid angle [4], and taking into account the designations introduced formerly [4,9] it can be presented as

$$\langle i(0)\rangle_\Omega = en^* S_z \frac{\langle v\rangle}{4}\langle \eta\rangle_\Omega , \tag{1}$$

where $S_z = 2\pi r_z l$ is the probe surface area, n^* is the probe-perturbed electron concentration, $i(0)$ is the current on the probe at the plasma potential ($V=0$), $\langle\ \rangle_\Omega$ is the solid angle average,

$$\eta = \mathrm{Is}_0(\alpha) + \alpha^2[\mathrm{Is}_0(\alpha) + \mathrm{Is}_1(\alpha)] ,$$

from which it follows (see Ref. [4])

$$\langle \eta\rangle_\Omega = \int_0^2 \mathrm{Is}_0(\alpha\sin\gamma)\,d\gamma + \alpha^2\int_0^{\pi/2}[\mathrm{Is}_0(\alpha\sin\gamma) + \mathrm{Is}_1(\alpha\sin\gamma)]\sin^3\gamma\,d\gamma , \tag{2}$$

where

$$\mathrm{Is}_n(\xi)=e^{-\xi^2/2}I_n(\xi^2/2) \tag{3}$$

and functions $I_n(x)$ (x is real, $x>0$) are known as the cylindrical functions of imaginary argument, $\alpha=v_d/v_0$, $v_0=(\sqrt{\pi}/2)\langle v\rangle$ is the most probable velocity for the Maxwellian distribution function, and γ is the angle between the probe axis and the vector $\mathbf{v}_d$.

Let us also consider the expression for the second derivative of the probe I-V characteristic, averaged over the solid angle, obtained from the theory [4]

$$\langle i''(x)_\Omega=eS_z v_0\frac{8\alpha^4}{\sqrt{\pi^3 x}}\int_0^\pi d\varphi(\sqrt{x}-\cos\varphi)\int_0^{\pi/2}d\gamma(\sin^5\gamma)e^{-\alpha^2\sin^2\gamma(\sqrt{x}-\cos\varphi)}\,, \tag{4}$$

where $x=2eV/mv_d^2$ and V is the probe potential.

The average velocity of the electron transport to the near-probe region [9] is determined in this case by the equation

$$\langle v_d\rangle_\Omega=\frac{\pi}{4}v_d \tag{5}$$

since the solid angular element is $2\pi\sin\gamma\,d\gamma$ and

$$\int_0^{\pi/2}d\gamma\sin^2\gamma=\frac{\pi}{4}\,.$$

Then the equation for calculating the probe-unperturbed electron concentration will have the form [9]

$$\xi^3+\xi^2\frac{r_z}{\lambda_s^*}\left[1+\frac{2}{\alpha\sqrt{\pi}}\langle\eta\rangle_\Omega\right]-\xi-\frac{r_z}{\lambda_s^*}=0\,, \tag{6}$$

where $\xi=\sqrt{n^*/n}$, n is the probe-unperturbed concentration of electrons, and

$$\lambda_s^*=\frac{v_s}{\sqrt{8\pi e^2 n^*/m}}$$

is introduced as some shielding length, resembling the Debye length, where the value $v_s(v_d,\langle v\rangle)$, as the function of v_d and $\langle v\rangle$, can be found from the experimental data, obtained from the simultaneous measurements by the probe pair, in the following way.

It has been shown [9] that a closed electric circuit of the probe measurements consists of three elements: a voltage generator (scanning generator with the voltage U_g), a linear resistor R_T ($R_T=R_p+R$, where R is the resistance of the interconnecting wires leading to the probe and R_p is the near-probe sheath impedance), and a nonlinear resistance of plasma with the drop in potential U_z. Therefore, for this circuit the following equation is true:

$$U_z=U_g-(R_p+R)i(U_g)\,, \tag{7}$$

from which it follows that the second derivative of the I-U_z characteristic with respect to voltage U_z is related to the second derivative of the I-U_g characteristic with respect to voltage U_g by the relation

$$\frac{\partial^2 i}{\partial U_z^2}=\frac{\partial^2 i}{\partial U_g^2}\left[1-R_T\frac{\partial_i}{\partial U_g}\right]^{-3}. \tag{8}$$

In Ref. [9] the relation has been found for the value R_p, which can be used here taking into account Eq. (5) and substituting λ_s for λ_D (λ_D is the Debye length):

$$R_p=9\times10^{11}\frac{2}{v_d}\frac{r_z+\lambda_s}{l}\left\{1-\frac{r_z}{r_z+\lambda_s}\left[1+2\ln\left[\frac{r_z+\lambda_s}{r_z}\right]\right]\right\}, \tag{9}$$

where R_p is given in Ω and the rest of the values are in electrostatic cgs (CGSE) units.

This model of the sheath impedance R_p is possible due to a velocity and space symmetry. However, the results obtained by Eq. (9) require additional tests.

For the sake of simplicity let us indicate the probe of 5-μm diam by the number 1, and that of 26-μm diam by the number 2, while all the values related to these probes will be supplied with the corresponding indices 1 and 2. Our task will consist in the computer selection of the resistance R_v in the electrical circuit of the probe 2 such that the resultant correcting to the derivatives of the I-V characteristics of this probe [with the help of Eqs. (8) and (9) after substituting R_v for R_T] would have a best fit to the second derivatives of the corresponding I-V characteristics from the probe 1 obtained in the same experiment.

A simple straightforward analysis of the considered electric circuit makes it possible to write down for the selected value of R_v the expression

$$R_v=(R_{p2}+R_2)-\frac{r_{z1}l_1}{4_{z2}l_2}(R_{p1}+R_1)\,. \tag{10}$$

Here the coefficient of $(R_{p1}+R_1)$ is due to the requirement of referring the electrical parameters of the circuits to a single concrete area of the probe surface. Substituting Eq. (9) into Eq. (10) we obtain the relation

$$R_v = R_2 - \frac{r_{z1} l_1}{r_{z2} l_2} R_1 + 9\times 10^{11} \frac{2}{v_d l_2} \left[\Psi(r_{z2}, \lambda_s) - \frac{r_{z1}}{r_{z2}} \Psi(r_{z1}, \lambda_s) \right], \tag{11}$$

where

$$\Psi(r_{zm}, \lambda_s) = (r_{zm} + \lambda_s) \left\{ 1 - \frac{r_{zm}^2}{(r_{zm} + \lambda_s)^2} \left[1 + 2 \ln \left[\frac{r_{zm} + \lambda_s}{r_{zm}} \right] \right] \right\}, \tag{12}$$

and m is the probe number. Relation (11) enables one to find the value of λ_s and to reconstruct the second derivatives of the I-V characteristics of both of the probes [with the help of Eqs. (7), (8), and (9)]. After their reconstruction we can by least square fitting to them the function $\langle i''(x) \rangle_\Omega$ [see Eq. (4)] to determine all parameters of the electrons in plasma: n, α, v_d, and v_0 [see Eqs. (1) and (6)], which presumably correspond to probe-unperturbed plasma. Note that using the described procedure in the practice enabled finding the scaling for determining value $V_s = mv_s^2/2e$ by the second derivative of the corrected I-V characteristic of the single probe, the sense of which is presented in Figs. 1(a) and 1(b). From Fig. 1(b) we see the physical sense of this scaling. Indeed, in the absence of the negative part of oscillogram $i''(U_z)$ one can assert that we observe the electron-distribution function which forms in velocity space the spherical layer with an energetical thickness V_s. As follows from this image, the value V_s is an equivalent measure of the thermal motion of the electron flows, which is averaged in solid angle for the cylindrical probe. This averaging is a result of different ratios of electron thermal velocity to the component of velocity $\mathbf{v}_d$ orthogonal to the probe surface, versus the different angles between the vector $\mathbf{v}_d$ and the probe axis. Note that $eV_s \geq m\langle v \rangle^2/2$ at $\alpha \geq 0$.

The identity of graphs $i_1''(U_z)$ and $i_2''(U_z)$ (see Fig. 5) compared after the reconstruction makes possible the statement that the Poisson equation for the near-probe layer [9] should be solved as $\Delta V = i(V) R_p(r_z, \lambda_s)$, where $R_p \neq \psi(V)$, and it proves the validity of Eq. (9). In Fig. 6 one can see the comparison of the reconstructed oscillograms $i''(U_z)$ with the graphs of the function $\langle i''(x) \rangle_\Omega$ determined by Eq. (4).

III. EXPERIMENTAL RESULTS

The peculiarities of the original plasma source configuration [1] hindered the use of the other plasma di-

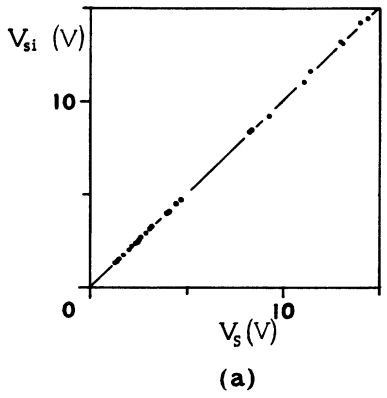

FIG. 1. (a) Comparison of value V_s which is determined from the experimental data processing, with the value V_{si} determined by the graph $i''(U_z)$. (b) The technique for obtaining the value of V_{si} by a graph $i''(U_z)$, $a = A \exp(-4/\pi)$.

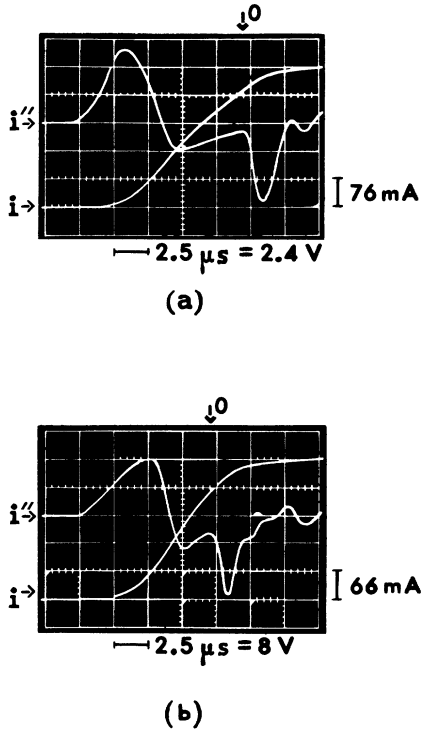

FIG. 2. (a) Oscillograms $i(U_g)$ and $i''(U_g)$ obtained at the plasma source [2], $r_z = 13$ μm, $l = 3.5$ mm. (b) Oscillograms $i(U_g)$ and $i''(U_g)$ obtained at the mirror machine [3], $r_z = 2.5$ μm, $l = 3.5$ mm.

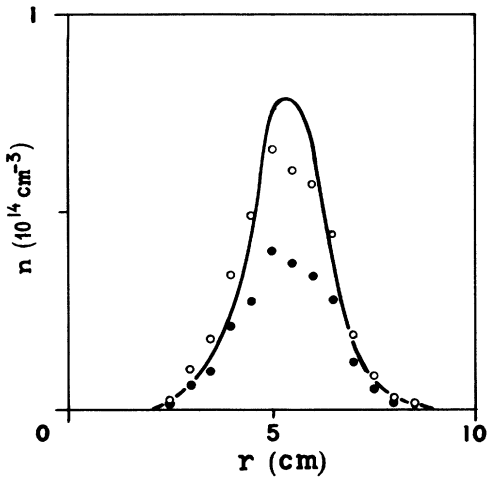

FIG. 3. The plasma-density distribution along the radius of the mirror machine. Symbols: (●) result of calculations without the reconstruction of the probe I-V characteristics; (○) result after the reconstruction. The solid line is the result of the multichord measurements by the hydrogen atomic beam.

agnostic methods required to verify this method. A special series of the experiments performed on another experimental installation (magnetic-mirror machine [2]) lacked this drawback. A single probe of 5-μm diam and ~3-mm length was used for the measurements (the probe configuration in this case was developed especially because of high potential instability in plasma studied [10]). The probe was inserted in the middle cross section of the mirror machine and provided the measurements of the plasma parameters distribution along the machine radius. In this series of the experiments the probe I-V characteristics and their derivatives at the midplane did not differ in shape from those obtained at the plasma source [1] [see Figs. 2(a) and 2(b)]. Two more types of diagnostics were used on the mirror machine for checking the probe measurements. One of them was the multichord probing by an atomic hydrogen beam [11], providing a detection of the plasma density distribution along the machine radius, and another one was the diagnostic providing the measurement of electron energy, averaged over the machine diameter, by an atomic argon beam [2]. Here and everywhere in this work we use the definition "temperature" only to correspond to the Maxwellian distribution function.

The distribution of the plasma density along the mirror-machine radius, obtained by the probe, is shown in Fig. 3 as the points. The solid points correspond to the direct calculation and the open points show the result of the reconstruction of plasma parameters. The data indicated in the same figure by the solid line were obtained by multichord probing. The agreement of the results for such different methods should be considered as satisfactory. The value of the average electron energy measured by the atomic argon beam, $\langle \epsilon \rangle = 10 \pm 1$ eV, agrees well with the value $m(v_d^2 + \langle v \rangle^2)/2e = 9.5 \pm 0.4$ eV calculated by the I-V characteristic of the probe. Note that combined changes of electron concentration and parameter v_s (see Fig. 1) along the mirror-machine radius in this case produced an effect similar to a conservation of constant scalar multiplier while reconstructing the electron concentration by Eq. (6); see Fig. 3.

Let us consider the most important results which were obtained at the plasma source [1]. Figure 4 shows the distribution of the electron concentration along the axis of source calculated from the I-V characteristics of the probes. In Fig. 5 the second derivatives of the I-V characteristics, $i_1''(V)$ and $i_2''(V)$, are given versus the distance from the source on its axis. Note that the resistance of the wire connected to the 26-μm-diam probe was 1 Ω, and the one connected to the 5-μm-diam probe was 25 Ω. As the result, the difference between the measured second derivatives of the I-V characteristics of these probes is not as significant as it could be at the equal resistances.

The analysis of Figs. 4 and 5 shows that the data obtained from the probes with different diameters coincide after the reconstruction. This result, together with the results of the investigations performed at the mirror machine, makes it possible to use reconstructed plasma parameters as the reliable material.

Let us consider the results of the two more experiments important for the comprehension of the problem studied. The probe pair with 5-μm and 100-μm diam, similar to that already considered, was inserted into plasma at the source [1]. The electron concentration and the shapes of $i''(V)$ obtained by the 100-μm-diam probe differed considerably from the ones obtained by the 5-μm-diam probe in the whole spectrum of the parameters studied (even after their reconstruction); see Fig. 4. Without going into detail about the measurements performed, let us consider the final conclusions resulting from them. An increase of the probe radius up to the dimension exceeding two shielding lengths, $r_z > 2\lambda_s$, results in the fatal alteration

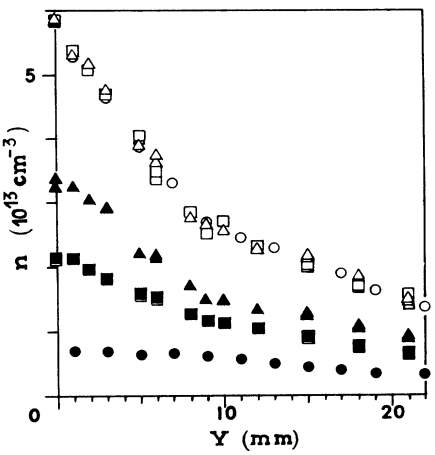

FIG. 4. The fragment of the electron concentration distribution along the plasma-source axis [2]. Symbols: (▲), (■) the data obtained from the probe pair of 5-μm and 26-μm diam, respectively; (△), (□) the same data after the reconstruction of the probe I-V characteristics; (○),(●) the data from the probe pair of 5-μm and 100-μm diam, respectively, after the reconstruction.

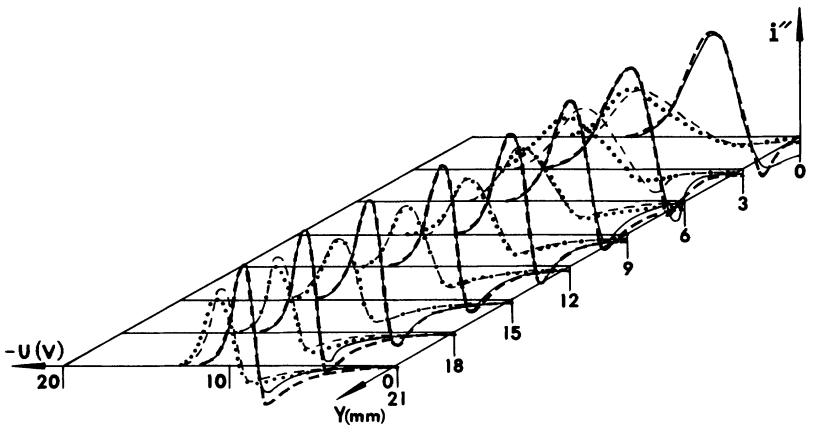

FIG. 5. The evolution of the second derivative of the probe I-V characteristic, $i''(V)$, along the axis of the plasma source [2]. The thin dashed lines indicate oscillograms $i''(U_g)$ from a 5-μm-diam probe; the dotted lines indicate oscillograms $i''(U_g)$ from a 26-μm-diam probe; the thin solid lines and the thick dashed lines are the result of the reconstruction of these oscillograms, respectively.

of both the parameters of the near-probe layer and the probe operation mode. The only reasonable explanation of this result can be discussed, namely the formation of the shock wave produced by supersonic flows interacting with the probe. Another important experimental fact is that the I-V characteristics of the probes were independent on the probe orientation on both the experimental installations [1,2]. However, the main result is the coincidence of the second derivatives of the probe I-V characteristics at plasma studied with the function determined by Eq. (4), $\langle i''(x)\rangle_\Omega$; see Fig. 6.

IV. ANALYSIS OF EXPERIMENTAL RESULTS

The experimental results support the assumption that there is filamentation of the isotropic thermal motion of electrons in the cases described here. This assumption was based on the fact that for the electron-distribution function, related to the laboratory coordinate system, $v_d \ll \langle v \rangle$, the second derivative of the probe I-V characteristic, $i''(V)$, cannot be negative within the interval $0 > V > V_f$, where V_f is the floating potential.

Here and further we shall use the definition in the correspondence to which the function sign is positive if it coincides with the sign of the probe current, $i(V)$. Let us prove that the mentioned assumption is correct if the near-probe layer potential is taken into account. Let the drop in potential applied to the plasma be expressed as $U_z = U_z(U_g, i)$; then the equation for the current on the probe will have the form

$$\frac{i}{enS_z} = \tfrac{1}{4}\int_{\sqrt{2eU_z/m}}^{\infty} f(v)v(1-2eU_z/mv^2)dv \ , \qquad (13)$$

from which it follows

$$\frac{i'}{enS_z} = -\frac{2e}{m}\frac{\partial U_z}{\partial U_g}\tfrac{1}{4}\int_{\sqrt{2eU_z/m}}^{\infty} dv\frac{f(v)}{v} \ , \qquad (14)$$

and then

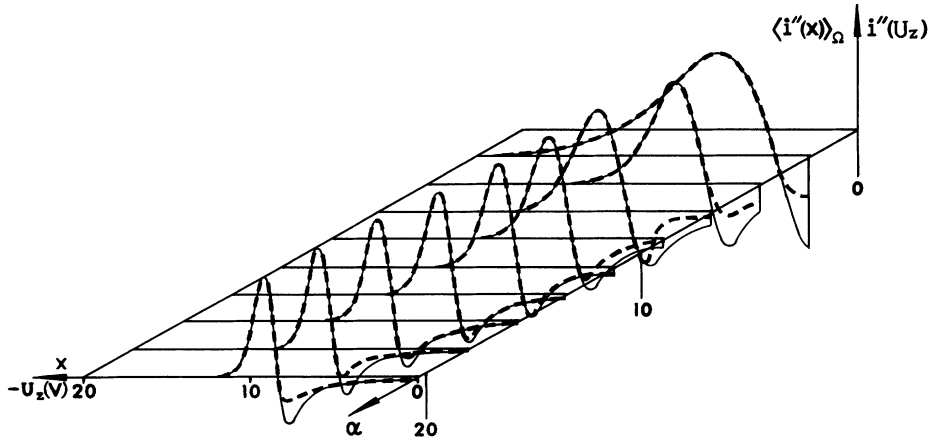

FIG. 6. The comparative shapes of reconstructed oscillograms $i''(U_z)$ (thick dashed lines) and the graphs of the function $\langle i''(x)\rangle_\Omega$ determined by Eq. (4) (thin solid lines).

$$\frac{i''}{enS_z}=\frac{e}{4m}\left[\frac{\partial U_z}{\partial U_g}\right]^2\frac{1}{U_z}f(\sqrt{2eU_z/m}\,)+\frac{\partial^2 U_z}{\partial U_g^2}\left[\frac{\partial U_z}{\partial U_g}\right]^{-1}\frac{i'}{enS_z}\ , \tag{15}$$

where $i'=\partial i/\partial U_g$, etc. Since the solution of the Poisson equation for the near-probe layer is given by the relations (see above)

$$U_z(U_g,i)=U_g-iR_p\ , \tag{16}$$

$$U_z'(U_g,i)=1-i'R_p\ , \tag{17a}$$

$$U_z''(U_g,i)=-i''R_p\ , \tag{17b}$$

then, substituting Eqs. (17a) and (17b) into Eq. (15), we obtain the equation

$$\frac{1}{U_z}f(\sqrt{2eU_z/m})=\frac{4m}{e^2nS_z}\frac{i''}{(1-i'R_p)^3}\ , \tag{18}$$

which is another form of expression (8). Since U_z is a monotonic function of U_g, its derivative cannot change its sign and i'' can be only positive; see Eqs. (17a) and (18).

Summing up all the above arguments and taking into account that the plasma potentials were found by the emissive probe with experimental accuracy to within ~ 0.2 V, we come to the conclusion that the only possible explanation of all of the experimental data is the assumption that the plasma electrons are arranged in separate flows. Each flow appears to be characterized by some temperature in the system reference frame to this flow, and directions of all the flows are distributed isotropically over the solid angle. Note that the effects of the secondary electron emission for the cleaned probe surface could be perceptible at electron energy >60 eV [7]. But as is seen from Figs. 2, 5, and 6, the considered range of electron energies is not more than ~ 12 eV, and the main phenomenon, namely the presence of the negative part of the *I-V* characteristic, occurs in a lower-energy range $\sim 2-6$ eV.

Let us consider some consequences of this conclusion. The reasonable mechanism causing the stratification of the isotropic thermal motion of electrons into the separate flows is the mechanism of the current instability [3]. In this case the condition of the plasma quasineutrality conservation, $\oint_s \mathbf{j}\,ds=0$ is reduced to the form $\sum_i \mathbf{i}_{ci}=0$, from which it follows, in the first approximation, that for every separate current of filament, $\mathbf{i}_{ci}$, there corresponds a current that is equal in magnitude and flowing in the opposite direction. To conserve this stratification and, consequently, to prevent mixing these electron flows at the exchanges of the flow directions, the pressure of the magnetic fields of these flows on their boundary should be equal to the kinetic pressure of these electron flows moving with the average velocity v_d. This condition can be written in the form

$$\frac{\mu H_c^2}{8\pi}=n\frac{mv_d^2}{2}\ . \tag{19}$$

Note that the thermal motion of electrons in the flow partially compensates for the magnetic field inside of the flow and displaces it to the flow boundary. This effect can be described in terms of plasma diamagnetism ($\mu<1$). However, the maximum found in the experiments at the mirror-machine [2] value of $\alpha\approx 2.3$, hence $\langle v\rangle^2/v_d^2=0.25$ [see Figs. 2(b) and 5], and we will consider the value of the magnetic field and its pressure just at the boundary of the flows where the thermal electron motion is negligible due to the process of self-contraction of each of the electron flows, and where consequently $\mu\sim 1$.

Let us assume that the magnetic field H_c is induced by a cylindrical current $i_c=\pi r_c^2 enc_d$; as a result we have

$$H_c=2\frac{2i_c}{cr_c}=\frac{4}{c}\pi r_c env_d\ . \tag{20}$$

The coefficient 2 in the right-hand side of Eq. (20) is due to the fact that the magnetic fields of the oppositely directed currents are added together on their mutual boundary. Substituting Eq. (20) into Eq. (19) we obtain

$$r_c=c/\sqrt{4\pi e^2 n/m}=c/\omega_{pe} \tag{21}$$

from which it follows that the length r_c is equal to the electron skin depth (here ω_{pe} is the electron plasma frequency).

There is an indirect corroboration of the validity of Eq. (21). The output aperture of the source [1] was changed during the process of optimization of the source parameters, and output plasma concentration was slightly decreased versus the increase of the aperture, corresponding to a decrease of the hydrogen pressure in the gas-discharge gap. However, the numerous attempts to decrease the output aperture less than ~ 2 mm led to a sharp decrease of output electron concentration to the value $\sim 10^{12}$ cm^{-3} at the aperture diameter ~ 1.6 mm. This blanking effect can be explained in the frames of our approach. Indeed, substituting the output electron concentration presented in Fig. 4 into Eq. (21) we obtain $r_c\approx 2$ mm, which corresponds to the conception that the single filament cannot leave the gas-discharge chamber due to conservation of the plasma quasineutrality. Thus, the assumption that $\mu\sim 1$ can be considered as the good approximation for our theory, at least in the application to plasma source [1], where $\langle v\rangle/v_d\ll 1$; see Figs. 5 and 6.

Since an arc discharge was used for the plasma generation in both the considered cases [1,2], let us assume [6] that plasma electrons at the source output are monoenergetic. For the values of n (see Fig. 4) and v_d ($mv_d^2/2e\approx 9$ eV; see Fig. 5) experimentally obtained at the plasma source [1], the length of electron scattering on ions is 3.6 cm, while the length of the source channel with the diaphragms is $L_d=3.5$ cm. Therefore, it should be expected that at the source output the electrons are scattered isotropically over the directions practically without the energy loss. Under these conditions the electrons form the thin spherical layer in velocity space. The length of electron scattering on ions was calculated from the relation [12,13]

$$\lambda^{ei}=\tau_1^{ei}v_d \ , \tag{22}$$

where

$$\tau_1^{ei}=\sqrt{m/2}\frac{4}{\pi e^4}\frac{\varepsilon^{3/2}}{n\lambda_c} \ . \tag{23}$$

Here λ_c is the Coulomb logarithm (in its calculation the Debye length was substituted by the value of λ_s) and the coefficient 4 in the right-hand side of Eq. (23) means that for the full isotropy of scattering, the electron should be scattered at the angle π.

The localized current is formed in velocity space by a segment with the solid angle,

$$\Omega_c=2\pi\int_0^{\beta}\sin\vartheta\, d\vartheta=2\pi(1-\cos\beta) \ ,$$

and the average directed velocity of electrons is determined by the relation (see Fig. 7)

$$v_d=\frac{2\pi}{\Omega_c}v_u\int_0^{\beta}\sin\vartheta\cos\vartheta\, d\vartheta \ ,$$

hence

$$v_d=\tfrac{1}{2}v_u(1+\cos\beta) \ . \tag{24}$$

The initial value of the maximum transverse velocity is

$$v_r=v_u\sin\beta \ . \tag{25a}$$

In this connection, the following statement is valid:

$$v_u=\lim_{\beta\to 0}v_d \ , \tag{25b}$$

since $\beta\to 0$ when $\alpha\to\infty$ ($\alpha=v_d/v_0$). Thus, the value of v_u found from the experimental data obtained at the plasma source [1] is $v_u=(17.5\pm0.5)\times10^7$ cm/s (see Figs. 8 and 5).

The switch-on of the magnetic field H_c can considerably affect the transverse velocity component and it is risky to determine it by a simple logical tracing. Nevertheless, the experimental data make it possible to obtain the functional dependence between the value $\cos\beta=2v_d/v_u-1$ [see Eq. (24)] and the value $\langle v\rangle/v_d=(2/\sqrt{\pi})/\alpha$, since the values of α, v_d, and v_u are known from the experiments. This dependence, determined for the whole range of investigated parameters, is presented in Fig. 8. As is seen from this figure, the relation

$$\langle v\rangle=\tfrac{1}{2}v_d(1-\cos\beta) \tag{26}$$

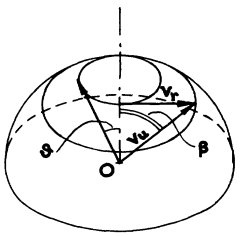

FIG. 7. Formation of a filament in velocity space.

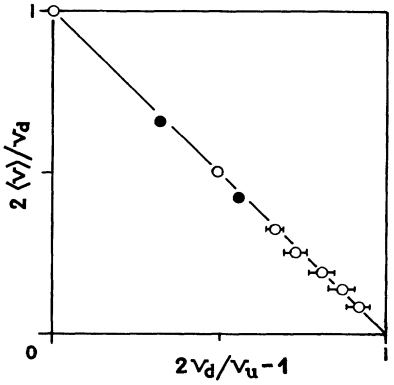

FIG. 8. The experimental relation between parameter $\alpha=(2/\sqrt{\pi})v_d/\langle v\rangle$ and the ratio v_d/v_u.

agrees well with the experimental data, hence

$$\sin\beta=\sqrt{1-(1-4/\alpha\sqrt{\pi})^2} \ . \tag{27}$$

It is natural to assume that the size r_c, determined by Eq. (21), is limited by the electron free-path length in the direction orthogonal to that of the current:

$$r_c\sqrt{2}=v_r\tau_1^{ei} \ . \tag{28}$$

The coefficient of r_c, $\sqrt{2}$, follows from the condition of conservation of plasma quasineutrality, i.e., after stratification each current filament will have to pass through an area two times smaller compared to that before the stratification.

A successive substitution of Eqs. (23), (25), and (21) into Eq. (28) results in the relation

$$\sin\beta=\sqrt{n}\frac{\sqrt{\pi}}{4}\lambda_c e^3 c[v_u\varepsilon_u^{3/2}]^{-1} \ , \tag{29}$$

where $\varepsilon_u=mv_u^2/2$.

Thus, if the value of v_u, entering in Eq. (29), is conserved along the source axis (the energy loss along the distance $L\sim5$ cm is negligible), then for the present particular case the dependence

$$\sqrt{1-(1-4/\alpha\sqrt{\pi})^2}=C\sqrt{n} \tag{30}$$

should hold true [see Eqs. (27) and (29)].

From Eq. (30) it follows that by plotting the values $[1-(1-4/\alpha\sqrt{\pi})^2]^{1/2}$ calculated from the experimental data as the ordinates, and the corresponding values $\sqrt{n}$ as the abscissa, we should obtain the experimental points on the line through the origin. The result of such a procedure is given in Fig. 9. The value of v_u, which was found with the help of Eq. (29) by the slope of the line crossing the experimental points in Fig. 9, $v_u=(15.5\pm0.3)\times10^7$ cm/s, agrees with the one found above from another consideration.

Despite the fact that the measurements at the plasma source [1] were performed at different distances from the source and at different modes of operation, from Fig. 9 it is clear that the experimental points do not strictly

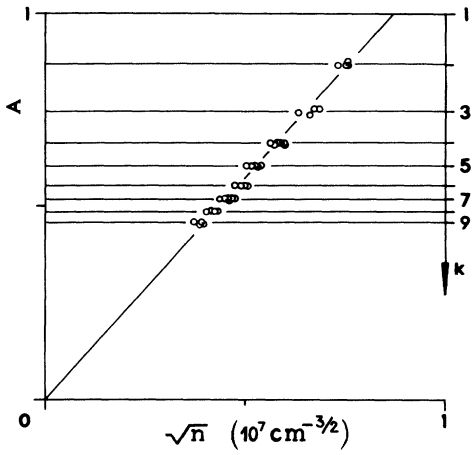

FIG. 9. The experimental dependence of parameter $A=[1-(1-4/\alpha\sqrt{\pi})^2]^{1/2}$ on the electron concentration n.

adhere to the line connecting them, but they form discrete groups for parameter α. This fact is not arbitrary and can be explained.

While stratifying the isotropic electron distribution, each of the currents obtained cuts out in velocity space a segment of the solid angle $\Omega_c=2\pi(1-\cos\beta)$ from the total solid angle, 4π. Due to the equivalence of these currents, the following relation should be satisfied:

$$\frac{4\pi}{2(1-\cos\beta)}=2k \ , \tag{31}$$

where k is an integer and the coefficient 2 is connected to the appearance of the filaments in the pair. Determining $\cos\beta$ from Eq. (26) and substituting it into Eq. (31) we obtain the expression for the discrete values of α:

$$\alpha_k=\frac{4}{\sqrt{\pi}}k \ . \tag{32}$$

In Fig. 9 the levels corresponding to the modes k are marked at the right-hand side of the graph on the ordinate. It is evident that the experimental points are grouped near these levels and Fig. 6 illustrates this fact as well. In particular, from Eq. (32) it follows that for the minimum possible mode, $k=1$, the value of $\alpha_1=2.26$ and this value was discovered while processing some oscillograms obtained at the mirror machine [2]; see Fig. 6.

As was already mentioned, the bulk of the measurements was performed by the probe with the axis oriented orthogonal to that of the source [1]. Therefore, during almost every measurement the probe interacted along its whole length, $l\sim 3$ mm, with the constant plasma density, and hence with the same mode. Nevertheless, when the probe axis was oriented parallel to that of the source, one could observe mixed modes of filaments. Note that two solid experimental points in Fig. 8 were obtained for the mixed modes.

It is necessary to point out here that after the filamentation process, half of the energy of each electron flow is transformed to energy of the magnetic field of the filament, as it follows from Eqs. (19), (20), (21), as well as from the condition of the quasineutrality conservation. Therefore, the initial value of the energy of electron isotropic thermal motion is $\varepsilon_{u0}\approx 2\varepsilon_u$. However, it is obvious that this fact does not change the results obtained above. Note also that the electron filamentation in the external magnetic field should lead to the appearance of the high instability of plasma, which has been observed at the mirror machine [2].

V. DISCUSSION OF RESULTS

Thus, the assumption that the isotropic thermal motion of electrons in the described cases is stratified into localized currents is provided by the following facts.

(i) Ideal coincidence of the oscillograms $i''(U_z)$ and the graphs of the function $\langle i''(x)\rangle_\Omega$ [see Eq. (4) and Fig. 6].

(ii) Good agreement of the functional dependence determined by Eq. (30) (between parameter α and electron concentration n) with the experimental data (see Fig. 9).

(iii) The discreteness of parameter α [see Figs. 6, 9, and Eq. (32)].

(iv) The possibility to explain in detail the evolution of the oscillogram $i''(V)$ vs the distance from the source [1] (see Fig. 5).

(v) The sharp change of the oscillogram $i''(V)$ and the value of electron concentration measured by the probe at the transfer from the condition $r_z<2\lambda_s$ to the condition $r_z>2\lambda_s$, which corresponds to the excitement of the shock wave in the case of supersonic electron flows, while in the case of isotropic thermal motion of electrons it cannot be observed (see Fig. 4).

On both the experimental installations studied [1,2] plasma was produced by an arc gas discharge, which presupposed a high monoenergy of the electrons leaving the near-cathode region of the sources. For the Maxwellian electron distribution function the filamentation phenomenon should not have been observed, since different groups of electrons with different energies had different scattering parameters (entering in this problem). On one of the installations [5], where sources (plasma generators) were used similar to those investigated in this paper [1,2], the author had occasionally observed the electron distribution function near the Maxwellian one. But the reasons for the change to such an operating mode are still uncertain.

ACKNOWLEDGMENTS

I would like to express my deep gratitude to B. V. Chirikov, B. N. Breizman, E. D. Bender, P. A. Bagryansky, and G. I. Dimov for the fruitful discussions in the course of the paper preparation. The experimental part of this work was performed in Institute of Nuclear Physics, 630090 Novosibirsk.

[1] V. I. Davidenko, G. I. Dimov, I. I. Morozov, and G. V. Roslyakov, Sov. Phys.—Tech. Phys. **28**, 160 (1983) [Zh. Tekh. Fiz. **53**, 258 (1983)].
[2] G. I. Dimov, A. A. Ivanov, and G. V. Roslyakov, Sov. J. Plasma Phys. **8**, 546 (1982) [Fiz. Plazmy **8**, 970 (1982)].
[3] B. B. Kadomtzev and A. V. Nedospasov, J. Nucl. Energy, Part C 230 (1960).
[4] E. V. Shun'ko, Phys. Lett. A **147**, 37 (1990).
[5] G. I. Dimov, Russ. J. Quest. At. Sci. Technol. **3**, 13 (1988).
[6] G. V. Roslyakov, thesis, INP Novosibirsk, 1988.
[7] P. A. Bagrayansky and E. V. Shun'ko, Sov. J. Instr. Tech. Exp. **2**, 166 (1986).
[8] V. S. Belkin, Sov. J. Instr. Tech. Exp. **2**, 158 (1984).
[9] E. V. Shun'ko, Phys. Lett. A **143**, 317 (1990).
[10] E. V. Shun'ko, Rev. Sci. Instrum. **61**, 2471 (1990).
[11] A. A. Ivanov, A. A. Kabantsev, and G. V. Roslyakov (unpublished).
[12] *Questions of Plasma Theory* (Moscow, 1963), Vol. 1.
[13] L. Spitzer, R. Astron. Soc. **100**, 396 (1940).

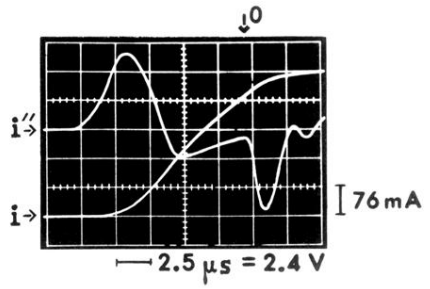

(a)

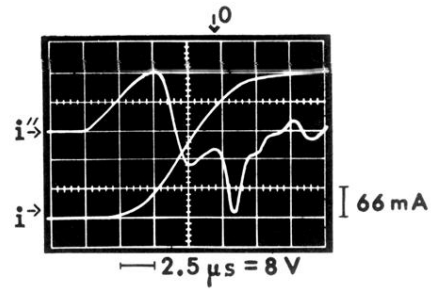

(b)

FIG. 2. (a) Oscillograms $i(U_g)$ and $i''(U_g)$ obtained at the plasma source [2], $r_z = 13$ μm, $l = 3.5$ mm. (b) Oscillograms $i(U_g)$ and $i''(U_g)$ obtained at the mirror machine [3], $r_z = 2.5$ μm, $l = 3.5$ mm.